and (1) are

$$\tau/\tau_w = 1 - Y \tag{25a}$$

$$\tau/\tau_w = 1 - (k\eta)^{-1} \tag{25b}$$

Expressing Eq. (18) in terms of ζ and eliminating $\ell_n R_\tau$ and U_c, we get

$$u = \tfrac{1}{2}U + u_\tau[k^{-1}\ell_n\zeta + \tfrac{1}{2}(B-D)] \tag{26}$$

which is an expression for velocity in the intermediate layer. This may be termed as a half-defect law. The expression for Reynolds stress in the intermediate layer obtained from Eqs. (1) and (26) is

$$\tau/\tau_w = 1 - R_\tau^{-\frac{1}{2}}[\zeta + (k\zeta)^{-1}] \tag{27}$$

It is seen that Reynolds stress in Eq. (27) is associated with a maximum, whose magnitude $\tau_{\max}$ and location $\zeta_{\max}$ are given by

$$\tau_{\max}/\tau_w = 1 - 2(kR_\tau)^{-\frac{1}{2}} \tag{28a}$$

$$\zeta_{\max} = k^{-\frac{1}{2}} \tag{28b}$$

V. Results and Discussion

The present three-layer analysis leads to the classical law of the wall, the velocity defect law, and the skin friction law. In the intermediate layer, the reference velocity is half of the velocity at the axis of the pipe/channel and the velocity distribution is governed by a half-defect law. From Eq. (26) it may be seen that $u \to U/2$, $\zeta \to \zeta_{\frac{1}{2}}$ where $\zeta_{\frac{1}{2}}$ is given by

$$\zeta_{\frac{1}{2}} = \exp[-\tfrac{1}{2}k(B-D)] \tag{29}$$

Taking $k = 0.41$, $B \simeq 5$, and $D \simeq 0.8$, Eq. (29) gives $\zeta_{\frac{1}{2}} = 0.42$ whereas the analysis[2] of data gives $\zeta_{\frac{1}{2}} = 0.44$. The data of Coantic[9] in terms of half-defect coordinates of Eq. (26) displayed in Fig. 1 show that substantial logarithmic regions with universal slope and intercept do in fact exist and that Eq. (26) can be represented by

$$(u - U/2)/u_\tau = 5.6 \log \zeta + 1.8 \tag{30}$$

A comparison of Reynolds stress expressions in Eqs. (25) and (27) with the data of Laufer is given in Fig. 4 of Ref. 2. The maxima in Reynolds stress predicted by Eq. (28b) at $\zeta_{\max} = 1.56$ is in better agreement with data[1,2] (1.85) when compared with $\zeta_{\max} = 1.54$ given by the mesolayer theory.[1] The difference in the theory and measurements can be caused by: 1) the maxima lies outside the logarithmic region in the intermediate layer; 2) the uncertainties in the location of maxima in the measured profile; and 3) uncertainties in measuring small distances, especially very close to the wall.

A comparison of the three-layer theory with the two-layer classical theory shows that the addition of the classical defect law [Eq. (17)] with classical law of the wall [Eq. (22)] leads to the half-defect law [Eq. (26)] for the intermediate layer. However, the similar addition of Reynolds stress expressions [Eqs. (25)] in the inner and outer layers produces an expression where terms of order $R_\tau^{-\frac{1}{2}}$ are different from the Reynolds stress equation (27) in the intermediate layer. This means that for the lowest-order results the two-layer classical theory should suffice as the intermediate layer forms the matching region between the classical two layers.[3,10] Therefore, there is no need to treat the intermediate layer through a separate expansion. However, for the first-order results, (i.e., $R_\tau^{-\frac{1}{2}}$), the intermediate layer is a distinct layer associated with the maximum value of Reynolds stress and it is necessary to consider the three-layer structure of the flow.[10]

Acknowledgment

The author is thankful to Dr. Shadbano Ahmad for critically reading the manuscript.

References

[1] Long, R. R. and Chen, T. C., "Experimental Evidence of the Existence of the Mesolayer in Turbulent Systems," *Journal of Fluid Mechanics*, Vol. 105, 1981, pp. 19-59.

[2] Afzal, N., "Fully Developed Turbulent Flow in a Pipe: An Intermediate Layer," *Ingen-Archiv*, Vol. 52, 1982, pp. 355-377.

[3] Afzal, N., "A Sub-Boundary Layer within a Two Dimensional Turbulent Boundary Layer: An Intermediate Layer," *Journal de Mécanique Théorique et Appliquée*, Vol. 1, 1982, pp. 963-973.

[4] Afzal, N. and Bush, W. B., "A Three Layer Asymptotic Analysis of Turbulent Channel Flow," (submitted to *Journal de Mécanique Théorique et Appliquée*).

[5] Coles, J. D., *Perturbation Methods in Applied Mathematics*, Blaisdell, Waltham, Mass., 1968.

[6] Van Dyke, M., *Perturbation Methods in Fluid Mechanics*, Academic Press, New York, 1964.

[7] Tennekes, H., "Outline for a Second-Order Theory of Turbulent Pipe Flow," *AIAA Journal*, Vol. 6, No. 9, Sept. 1968, pp. 1735-1740.

[8] Coles, D. and Hirst, E. A., "The Computations of Turbulent Boundary Layer," *Proceedings of 1968 IFP-AFOSR-Stanford Conference*, Vol. 2, Stanford University Press, 1969, pp. 1-54.

[9] Coantic, M., "Evolution, en fonction due nombre de Reynolds de la distribution des vitesses Moyennes et turbulentes dans une conduite," *Comptes Rendus de Academic des Sciences, Paris*. Vol. 264, 1967, pp. 849-852.

[10] Afzal, N., "Three Layer Theory of a Turbulent Boundary Layer on a Flat Plate," *Proceedings of the Second Asian Congress of Fluid Mechanics*, Science Press, Beijing, 1983, pp. 316-321.

An Enhanced Flow Visualization Technique for Planar Free Shear Layers

Y. Hsia,* D. Baganoff,† A. Krothapalli,‡ and K. Karamcheti§
Stanford University, Stanford, California

SCHLIEREN flow visualization has played an important role in the study of organized vortical motions in free shear layers.[1,2] This Note deals with a schlieren technique that enables one to visualize and identify specifically those fluid elements making up the shear layers in a plane jet. The enhanced visualization is achieved with the method by heating the reservoir gas (air) to a particular temperature according to the jet exit Mach number.

A rectangular nozzle of aspect ratio 16.7 (50 mm long, 3 mm wide) was used in the study. For the conditions of interest, hot-wire measurements showed that the flow was very nearly two-dimensional at the jet exit.[3] The flow facility allowed steady conditions to be realized for an hour or longer. Provisions were made to vary the reservoir air temperature by as much as 30°C above the ambient. A conventional schlieren system has been used with a spark light source. All schlieren pictures were taken with spark durations of 2.5 μs.

Received July 19, 1982; revision received July 7, 1983.

*Graduate Student, Joint Institute for Aeronautics and Acoustics. Student Member AIAA.

†Professor, Joint Institute for Aeronautics and Acoustics. Member AIAA.

‡Associate Professor, Dept. of Mechanical Engineering, Florida State University. Senior Member AIAA.

§Professor and Director, Joint Institute for Aeronautics and Acoustics. Fellow AIAA.

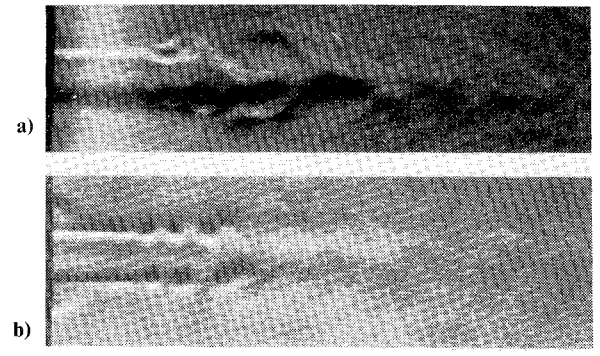

Fig. 1 Schlieren photographs of an air jet at an exit Mach number equal to 0.3 and for two different reservoir temperatures.

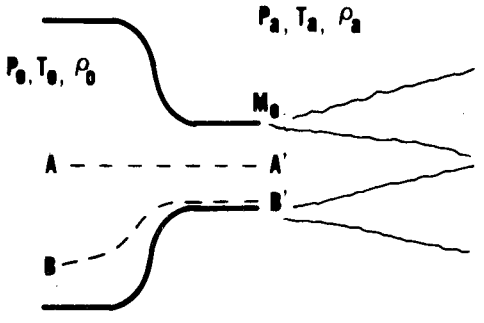

Fig. 2a Schematic of a jet emerging from a convergent nozzle (AA′ and BB′ represent two streamlines).

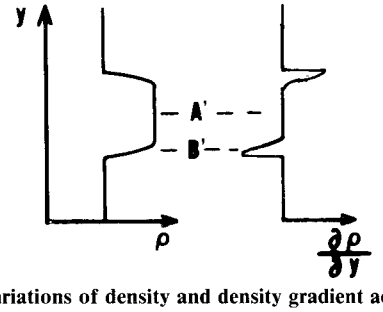

Fig. 2b Variations of density and density gradient across the nozzle exit for a nonheated jet.

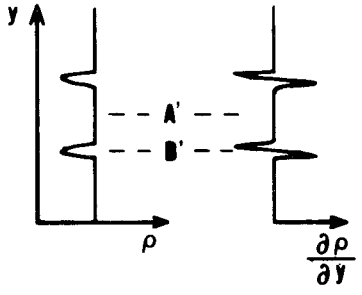

Fig. 2c Variations of density and density gradient across the nozzle exit for a properly heated jet.

Schlieren photographs of an air jet issuing from the rectangular nozzle at an exit Mach number equal to 0.3, obtained for two different reservoir air temperatures, are shown in Fig. 1. Figure 1a shows a photograph obtained with the conventional method. The corresponding picture obtained with the present method is shown in Fig. 1b. The resolution of these photographs is somewhat limited because of the low subsonic jet velocities and the resulting small density gradients. However, the main features of the shear layers can be seen clearly in Fig. 1b. The shear layers appear to be

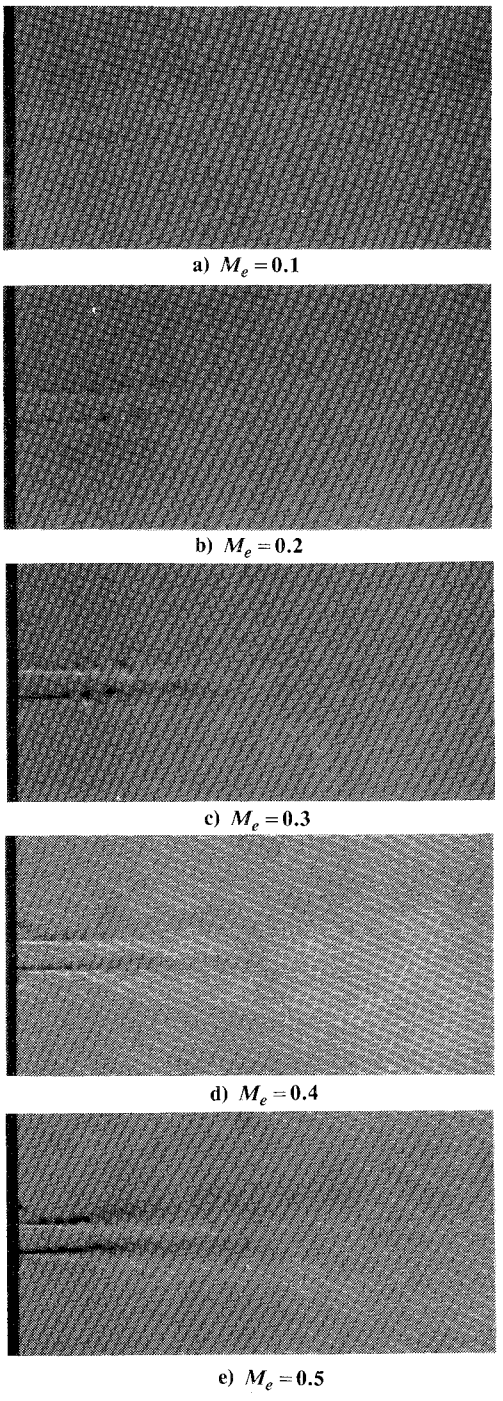

Fig. 3 Schlieren photographs of jet at various exit Mach numbers.

isolated from the jet body and can be studied as independent entities. Large-scale vortices, vortex pairing, and the intervening region between the two merging shear layers can be clearly discerned. The clear view of the individual vortices allows one to obtain quantitative information on the dynamics of vortex interaction, such as shedding frequency, separation distance, etc. The two fillets seen at the nozzle exit and outside the jet are believed to be the wakes of the nozzle lips. The thickness of each lip is 1.7 mm compared with the 3 mm width of the nozzle. Although heating has been used previously in conjunction with the schlieren technique to visualize flows,[1] the approach described here is to select a particular reservoir temperature to enhance a particular feature of the flow as depicted in Fig. 1b. In effect, the method provides a new view rather than a clearer image of a familiar view.

The method is described as follows. A flow of air emerging from a convergent nozzle (Fig. 2a) can be divided into two regions: a large region of inviscid flow represented by the central streamline AA′ and a thin viscous region near the wall represented by streamline BB′. A fluid particle which moves from A to A′ undergoes isentropic changes, while a particle traveling along BB′ undergoes nonisentropic changes. If the reservoir temperature is uniform, i.e., $T_A = T_B$, then the temperature at B′ is higher than that at A′ and the density at B′ is lower than that at A′. The temperature at A′, $T_{A'}$, can be determined using the isentropic relation

$$T_{A'} = T_0 [1 + (\gamma - 1)/2 \cdot M_e^2]^{-1} \quad (1)$$

where T_0 is the reservoir temperature, M_e the jet exit Mach number, and γ the specific heat ratio. Since M_e is greater than zero, $T_{A'}$ is always less than T_0. In most aerodynamic experiments, the reservoir temperature is kept the same as the ambient temperature (T_a), i.e., $T_0 = T_a$. Therefore, $T_{A'}$ is less than T_a. As a result, the density at A′, $\rho_{A'}$, is greater than the ambient density ρ_a because the static pressure at the jet exit is equal to the ambient pressure. The variations of density and density gradient across the jet exit are sketched in Fig. 2b. The density gradient profile represents the contrast in the schlieren picture (Fig. 1a). The present method is to adjust T_0 according to Eq. (1) so that $T_{A'}$ is equal to T_a and then $\rho_{A'}$ is also equal to ρ_a. However, the temperature at B' is still higher than $T_{A'}$ and the density at B′ is lower than $\rho_{A'}$. The resulting density and its gradient across the jet exit are sketched in Fig. 2c. Comparing the two density gradient profiles (Figs. 2b and 2c), it is seen that the present method (Fig. 2c) produces a larger variation of density gradient in the shear layer, which results in a sharper image. It is noted that the density gradient shown in Fig. 2c is similar to the second derivative of the density profile in Fig. 2b, which gives the greater visual appeal of the shadow effect. However, the schlieren method is known to be superior to the shadowgraph due to its higher sensitivity and better focusing ability. Therefore, the enhancement obtained with the method described is that it makes use of the best features of both the shadow and schlieren methods.

This method has been used successfully to obtain schlieren photographs of the jet at exit Mach numbers of 0.1-0.5 (see Fig. 3). The particular reservoir temperatures required for these conditions are 0.6-15°C above ambient. The corresponding density changes are less than 5% of the reservoir air density. Due to the small changes in temperature and density required by the method, it is expected that no significant effects of heating on flow properties, such as the jet velocity distribution, spreading rate, and heating of the ambient air, would be encountered.

Acknowledgment

This work was supported by the Air Force Office of Scientific Research, Contract F49620-79-0189.

References

[1] Moore, C. J., "The Role of Shear-Layer Instability Waves in Jet Exhaust Noise," *Journal of Fluid Mechanics*, Vol. 80, Pt. 2, 1977, pp. 321-367.

[2] Crow, S. C. and Champagne, F. H., "Orderly Structure in Jet Turbulence," *Journal of Fluid Mechanics*, Vol. 48, Pt. 3, 1971, pp. 547-591.

[3] Hsia, Y., Krothapalli, A., Baganoff, D., and Karamcheti, K., "The Structure of a Subsonic Compressible Rectangular Jet," Joint Institute for Aeronautics and Acoustics, Stanford University, Stanford, Calif., Rept. TR-43, Jan. 1982.

Ignition in Gun Exhaust Plumes

E. M. Schmidt*
Ballistic Research Laboratory, USAARRADCOM
Aberdeen Proving Ground, Maryland

Introduction

SECONDARY combustion is an undesirable signature of both gun and rocket plumes. While the latter are generally steady exhausts from two-dimensional, supersonic nozzles with moderate underexpansion, gun plumes[1] are transient and issue sonically at high pressure from the weapon muzzle. In addition, cannon frequently employ three-dimensional nozzles, called muzzle brakes, to reduce recoil. This Note examines the influence of both transient and three-dimensional flow on the probability of ignition in gun plumes.

Potential sources of ignition include viscous heating in lateral shear layers, hot particles, burning propellant grains, or tracers in the base of the projectile; however, experiments by Carfagno[2] point out the importance of the propellant gas recompression through the large Mach disks typical of gun plumes. Based upon his results, Carfagno proposes a model that assumes a one-dimensional expansion through a normal shock to ambient pressure followed by steady mixing with the surrounding air. The properties of the propellant gas/air mixture are assumed to be a uniform function of the mass of air entrained in the plume, permitting the mixture temperature to be defined as

$$\bar{T} = [rC_{p_\infty} T_{s_\infty} + (1-r) C_{p_1} T_{s_1} - (1-r)^2 u_1^2/2] / [rC_{p_\infty} + (1-r) C_{p_1}] \quad (1)$$

$$r = m_\infty / (m_\infty + m_1) \quad (2)$$

Carfagno makes no attempt to evaluate the details of the mixing process, but assumes that all values of r between zero and one are permissible. Ignition occurs when the local mixture temperature, $\bar{T}$, exceeds certain limits. The limits are established in shock tube experiments using various combinations of air and combustion products as test gases. The ignition temperature limits are relatively insensitive to propellant composition and mixture ratio for $0.2 < r < 0.8$; however, significant changes are associated with the addition of relatively small amounts of flash suppressants, such as potassium sulfate or nitrate (Fig. 1).

Yousefian[3] uses finite difference computations to analyze the mixing and chemistry in the gun plume downstream of the Mach disk. To obtain initial conditions, empirical correlations define the inviscid shock structure of the plume. The axial location of the Mach disk is that given by

$$X/D = 0.69(\gamma p^*/p_\infty)^{1/2} \quad (3)$$

Using a relation derived from core flow computations, the shock Mach number is obtained by interpolation of

$$(X/D)^2 = 0.49\gamma [2 + (\gamma - 1) M^2]^{\gamma/(\gamma-1)} [\gamma + 1]^{-1/\gamma - 1} \div [2\gamma M^2 - (\gamma - 1)] \quad (4)$$

Presented as Paper 81-1109 at the AIAA 16th Thermophysics Conference, Palo Alto, Calif., June 23-25, 1981; received Dec. 21, 1982; revision received June 20, 1983. This paper is declared a work of the U.S. Government and therefore is in the public domain.

*Supervisory Aerospace Engineer, Launch and Flight Division. Associate Fellow AIAA.